Spatial difference can occur between activated and damaged muscle areas following electrically-induced isometric contractions

Alexandre Fouré, Arnaud Le Troter, Augustin C. Ogier, Maxime Guye, Julien Gondin, David Bendahan

▶ **To cite this version:**

Alexandre Fouré, Arnaud Le Troter, Augustin C. Ogier, Maxime Guye, Julien Gondin, et al.. Spatial difference can occur between activated and damaged muscle areas following electrically-induced isometric contractions. The Journal of Physiology, 2019, 597 (16), pp.4227-4236. 10.1113/JP278205 . hal-02438449

HAL Id: hal-02438449
https://hal.science/hal-02438449v1

Submitted on 6 Sep 2024

HAL is a multi-disciplinary open access archive for the deposit and dissemination of scientific research documents, whether they are published or not. The documents may come from teaching and research institutions in France or abroad, or from public or private research centers.

L'archive ouverte pluridisciplinaire **HAL**, est destinée au dépôt et à la diffusion de documents scientifiques de niveau recherche, publiés ou non, émanant des établissements d'enseignement et de recherche français ou étrangers, des laboratoires publics ou privés.

Spatial difference can occur between activated and damaged muscle areas following electrically-induced isometric contractions

Alexandre Fouré[1,2,3], Arnaud Le Troter[1], Augustin C. Ogier[4], Maxime Guye[1,2], Julien Gondin[1,5] and David Bendahan[1]

[1] *Aix-Marseille Université, CNRS, CRMBM, UMR 7339, 13385 Marseille, France*
[2] *APHM, Hôpital Universitaire Timone, CEMEREM, 13005 Marseille, France*
[3] *Université de Lyon (UCBL1), Laboratoire Interuniversitaire de Biologie de la Motricité, EA7424, Villeurbanne, France*
[4] *Aix-Marseille Université, Université de Toulon, CNRS, LIS UMR 7020, 13385 Marseille, France*
[5] *Institut NeuroMyoGène, Université de Lyon (UCBL1), CNRS 5310, INSERM U1217, Lyon, France,*

Edited by: Janet Taylor & Karyn Hamilton

Key points

- T_2 mapping combined to image registration and statistical parametric mapping analysis is a suitable methodology to accurately localize and compare the extent of both activated and damaged muscle areas.
- Activated muscle areas following electrically-induced isometric contractions are superficial, but damaged regions are muscle specific and can be related to the muscle morphology and/or the relative spatial position within a muscle group leading to potential intramuscular muscle shear strain.
- Tissues other than active skeletal muscle fibres can be altered during unaccustomed neuromuscular electrical stimulation-induced isometric contractions.

Abstract Skeletal muscle isometric contractions induced by neuromuscular electrical stimulation (NMES) exercise can generate damage within activated muscles. This study aimed at comparing the localization and the extent of NMES-activated muscle areas and induced damage regions using magnetic resonance imaging. Thirteen healthy subjects performed a single bout of NMES-induced isometric contractions known to induce a decrease in maximal voluntary isometric contraction (MVC) and increase in muscle volume and transverse relaxation time (T_2). All the parameters were measured before, immediately after (POST), 7 days (D7), 14 days (D14) and 21 days (D21) after the NMES session. Spatial normalization of T_2 maps were performed to compare the localization of muscle activation areas and damaged muscle regions from statistical mapping analyses. A significant decrease in MVC was found at POST ($-26 \pm 9\%$) and in delayed time at D7

Alexandre Fouré received his PhD in sports sciences from the University of Nantes, France in 2010. He studied the effects of exercise-induced damage on muscle structure and metabolism using magnetic resonance imaging and spectroscopy during a postdoctoral period at the CRMBM-CEMREM Lab (Aix-Marseille University, CNRS, APHM). Since 2018 he has been an associate professor at the University Claude Bernard Lyon 1 (France) in the Sport Performance and Injury Prevention team of the 'Laboratoire Interuniversitaire de Biologie de la Motricité' (LIBM). Alexandre's research focus lies on the investigation of neuromuscular function, and muscle–tendon mechanical and structural properties especially in the context of muscle damage.

DOI: 10.1113/JP278205

(−20 ± 6%) and D14 (−12 ± 5%). Although muscle activation was statistically detected through T_2 increase at POST in superficial parts of the two muscles located beneath the stimulation electrodes (i.e. vastus lateralis and vastus medialis), alterations quantified in a delayed time from increased T_2 were mainly located in the deep muscle region of the vastus lateralis (+57 ± 24% of mean T_2) and superficial area of the vastus medialis (+24 ± 16% of mean T_2) at D7 and were still observed in whole muscle at D21. The discrepancy between activated and damaged areas in the vastus lateralis implies that tissues other than active skeletal muscle fibres were altered during unaccustomed NMES-induced isomeric contractions.

(Resubmitted 22 May 2019; accepted after revision 27 June 2019; first published online 28 June 2019)
Corresponding authors A. Fouré, Centre de Résonance Magnétique Biologique et Médicale (CRMBM), UMR CNRS 7339, Faculté de Médecine la Timone, 27 Boulevard Jean Moulin, 13385 Marseille, France. Email: alexandre.foure@hotmail.fr; J. Gondin, Institut NeuroMyoGène (INMG), CNRS 5310–INSERM U1217–UCBL1, Faculté de Médecine et de Pharmacie, 8 Avenue Rockefeller, 69008 Lyon, France. Email: julien.gondin@univ-lyon1.fr

Introduction

Neuromuscular electrical stimulation (NMES) has been shown to induce severe muscle damage under isometric conditions at long muscle length (Mackey *et al.* 2011; Nosaka *et al.* 2011; Fouré *et al.* 2015*a*,*b*). Within the days following this type of damaging exercise, structural alterations (Mackey *et al.* 2008, 2011) have been assessed in the muscles located beneath the stimulation electrodes. These findings have been supported by muscle transverse relaxation time (T_2) mapping using magnetic resonance imaging (MRI) (Fouré *et al.* 2015*a*). Surprisingly, T_2 increases in muscles directly located beneath the stimulation electrodes were reported as muscle-specific for knee extensors (Fouré *et al.* 2015*b*) and localized in the superficial part of the vastus medialis (VM) and the deep part of the vastus lateralis (VL).

In contrast to what occurs during voluntary contractions, the motor units' recruitment during electrically-evoked contractions is synchronous, spatially fixed and involves fast and slow motor units at the same time (Maffiuletti, 2010). The activation of fast muscle fibres even at relatively low levels of evoked force (Gregory & Bickel, 2005) can induce early fatigue and then generate fibre alterations. Although muscle activation is considered to be mainly superficial using NMES, MRI investigations have demonstrated a relative spatial heterogeneity regarding T_2 changes (Adams *et al.* 1993).

Two main contributing causes could be linked to these corresponding muscle tissue alterations. Direct damage could be generated in weaker sarcomeres during repeated muscle fibre activation associated with NMES similar to what has been suggested during voluntary eccentric exercise-induced muscle damage (Morgan, 1990; Proske & Allen, 2005). Indirect damage could occur as a result of an intramuscular strain and potential shear stress between active and passive parts within the stimulated muscles (Fouré *et al.* 2015*a*,*b*). This latter assumption is supported by muscle cell cytoskeletal alterations and extracellular matrix de-adhesion which have been reported after isometric NMES contractions (Mackey *et al.* 2008, 2011). In order to distinguish these potential causes, one had to determine the exact localization and extent of activated and damaged muscle areas resulting from NMES. On that basis, T_2 changes occurring immediately after NMES can be considered as the result of muscle activation (Adams *et al.* 1993; Fouré *et al.* 2017) whereas long-lasting T_2 changes reflect muscle alterations (Fleckenstein *et al.* 1989). T_2 mapping performed immediately and within days after NMES might provide key information as long as the issue of 3-D co-registration of magnetic resonance (MR) images can be addressed (Fouré *et al.* 2015*b*, 2018).

Therefore, the aim of the present study was to compare the localization of activated and damaged muscle areas after a NMES session on the basis of a robust spatial normalization of MRI datasets and using a statistical parametric mapping analysis. A superficial activation of muscles located beneath the stimulation electrodes and a muscle-specific localization of alterations in the following days after the NMES session was hypothesized.

Methods

Ethical approval

Subjects were fully informed about the nature and the aim of the study and gave their informed written consent to participate. This study was approved by the Local Human Research Ethics Committee (Sud Mediterranée V, no. 2012-04 A00449-34) and conducted in conformity to the standards set by the latest revision of the *Declaration of Helsinki*, except for registration in a database.

Subjects

Thirteen healthy subjects (26 ± 3 years, 173 ± 8 cm, 70 ± 9 kg, 4 women) volunteered to participate in this study. None of them was engaged in any training or exercise programmes. Subjects were instructed to

avoid any intensive and non-familiar physical activities throughout the duration of the protocol. Subjects were asked to keep their diet habits and limit their alcohol consumption throughout the study period. They were instructed to avoid consuming caffeine and smoking before experimentations. Consumption of medication was prohibited during the experimental protocol. All testing sessions were performed at the same time of day before (PRE) and immediately after the damaging exercise (POST) and then 7 days (D7), 14 days (D14) and 21 days (D21) after the first exploration as detailed in Fig. 1.

NMES session

Subjects were seated on a chair (Multi-Form', La Roque d'Anthéron, France) customized with a force sensor. Adjustable belts were used to secure hip and ankle joints to hold the hip and knee joints at 90° and 100°, respectively (0° corresponding to the joint fully extended). The right leg was stimulated using three electrodes placed over the thigh, one 5 cm × 10 cm on the proximal part of the thigh (i.e. placed ∼5 cm below the inguinal ligament) and two 5 cm × 5 cm positioned on the vastus lateralis (VL) and vastus medialis (VM) muscle bellies. Biphasic symmetric rectangular pulses were delivered at a frequency of 100 Hz with a pulse duration of 400 μs (40 contractions, 5 s on and 35 s off throughout the NMES session) using a portable battery-powered stimulator (Compex Performance, DjoGlobal, Mouguerre, France). Stimulation intensity was gradually increased while electrically-evoked force was measured during the NMES session and normalized to maximal voluntary contraction (MVC) force as previously described (Fouré *et al.* 2014, 2015*a*).

Maximal voluntary isometric contraction force

Each subject was seated on a chair with the knee flexed at 100° (full extension = 0°) and performed a 5–10 min warm-up including a set of submaximal knee extensions under isometric conditions. Subjects were instructed to perform three unilateral isometric MVCs with the right leg. The MVC trials were separated by a resting period of at least 30 s and the MVC value was considered as the highest value among the three trials.

MR image acquisition and post-processing

Subjects were positioned supine with the right leg centred in a 1.5-T super-conducting magnet (MAGNETOM Avanto, Siemens AG, Healthcare Sector, Erlangen, Germany). A flexible 6-channel coil (Siemens AG) was placed around the thigh. Muscle volume was determined from high-resolution T_1-weighted images (20 slices, field of view (FOV) = 220 mm × 220 mm; matrix = 576 × 576; TR = 549 ms; TE = 13 ms; number of repetitions (N_{EX}) = 1; slice thickness = 6 mm; gap between slices = 6 mm, acquisition time = 5 min 18 s). T_2-weighted images were acquired with a segmented (15 segments) echo planar imaging sequence with TE = 15, 25, 35, 45 and 55 ms. Other acquisition parameters were as follows: FOV = 220 mm × 220 mm; matrix = 192 × 192; TR = 4800 ms; N_{EX} = 1; number of slices = 20; slice thickness = 6 mm; gap between slices = 6 mm, fat saturation; acquisition time = 5 min 10 s. The most distal slice was always acquired at approximately 20 mm (i.e. 5% of the thigh length measured for each subject) above the proximal border of the patella. The stimulation electrodes were carefully localized by using oil capsules positioned on the skin surface. These capsules were visible on T_1-weighted images as circular hyper-signals on slices 3 ± 1 and 14 ± 1 for VM and VL, respectively.

Muscle volume and T_2 mapping. Regions of interest were drawn with FSLView (FMRIB, Oxford, UK) on the basis of a manual delineation of muscle boundaries for VL, VM, vastus intermedius (VI), rectus femoris (RF), sartorius (SAR), gracilis, adductor longus, adductor magnus, the

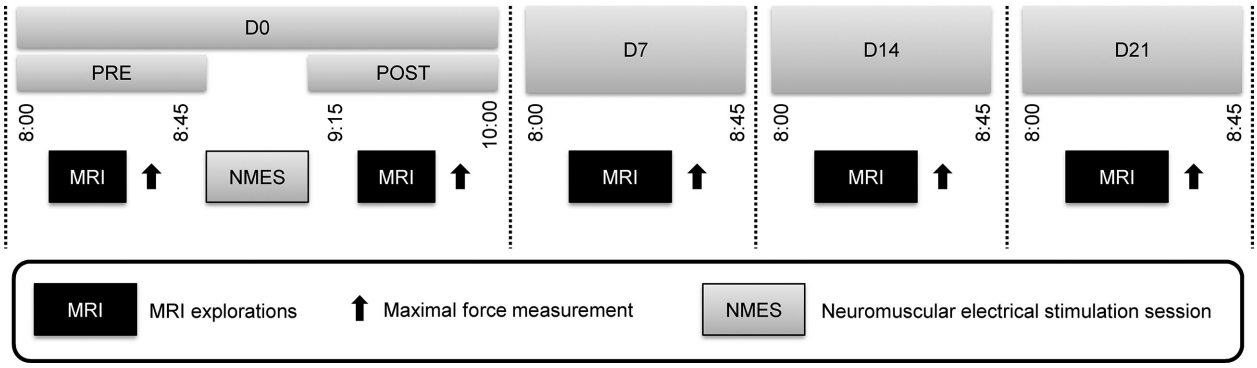

Figure 1. Schematic representation of the experimental design

two heads of the biceps femoris, semitendinosus and semimembranosus muscles. This delineation was performed for one every two slices and missing slices were automatically interpolated (Ogier *et al.* 2017). Using the truncated cone formula, muscle volume was calculated by summing the areas of all the slices, taking into account the slice thickness and the gaps between slices. Whole muscle T_2 maps were generated by a linear fit on a pixel-by-pixel basis (Fouré *et al.* 2015*a*, 2017) using the following equation:

$$\ln(S(TE)) = \ln(S_0) - (TE/T_2) \quad (1)$$

where S(TE) is the signal at time equal to TE and S_0 is the equilibrium magnetization. Regions of interest initially drawn on T_1-weighted images were used to analyse T_2 maps and to determine a mean T_2 value for each muscle.

Spatial normalization of the T_2 maps. As previously described (Fouré *et al.* 2015*b*), a multi-step method was performed for intra- and inter-subject normalizations using Advanced Normalization Tools (ANTs library). Both intra- and inter-subject normalizations were partly based on anatomical landmarks manually selected on T_1-weighted images. Landmarks-based 3-D warp deformation fields were used to impose strong constraints in order to increase the accuracy of the previous reported method (Le Troter *et al.* 2016).

First, T_1-weighted images and segmentation masks at POST, D7, D14 and D21 were deformed on PRE images and masks (i.e. targets) for each subject using non-linear registration processes. PRE images and masks of a single subject were extracted from the database and considered as the target of inter-subject normalization.

Each deformable field obtained from the intra- and inter-subject normalization processes was then applied on the corresponding T_1-weighted images, T_2 maps and segmentation masks, to warp all images in the common referential. Nearest-neighbour interpolation was applied to keep the integer values of the original labels of the segmentation masks.

The Dice similarity coefficient (DSC) (Zou *et al.* 2004) was used to estimate the overlap between muscle segmentations of each muscle for each subject over time (i.e. intra-subject normalization) and between subjects (i.e. inter-subject normalization).

T_2 quantification in deep and superficial parts of the VM and VL muscles. Two depth levels (i.e. superficial and deep) were considered for VM and VL the most damaged muscles located beneath the stimulation electrodes (Fouré *et al.* 2015*b*). As previously described, a polar co-ordinate system (with the bone centre used as the reference) was used to determine the thickness of damaged muscles at different angles and the frontiers between superficial and deep parts were then characterized in each slice (Fouré *et al.* 2015*b*). Regarding muscle length, three levels were considered (i.e. distal, slices 1–7; central, slices 8–13; and proximal, slices 14–20). T_2 was then quantified for each region and at each time point.

Statistics

Normality of the data distribution was initially investigated using the Shapiro–Wilk test. One-way ANOVA (time) was used (Statistica, StatSoft Inc., Tulsa, OK, USA) to assess immediate (i.e. PRE *vs.* POST) and remaining (i.e. PRE *vs.* D7–D21) changes in volume and T_2 of each muscle. Statistical parametric mapping (SPM) was performed using SPM12 (Wellcome Institute, London, UK) in order to compare on a pixel-by-pixel basis T_2 values across the whole set of subjects and the corresponding time-dependent changes for clusters larger than 100 voxels and $P = 0.0001$.

In addition, two-way ANOVAs (muscle depth × time) were used to assess T_2 differences between superficial and deep parts over time for both VL and VM and so for each muscle length level (i.e. proximal, central and distal). A Tukey's HSD *post hoc* analysis was performed when appropriate. The number of subjects was determined on the basis of a statistical power calculation ($\alpha = 0.05$ and $1 - \beta = 0.9$) and previous measurements (Fouré *et al.* 2015*a*) to detect a 6.3% T_2 increase for the whole quadriceps femoris.

Results

NMES session

Stimulation intensity was gradually increased throughout the 40 electrically-evoked contractions and reached 66 ± 16 mA (Fig. 2*A*). Peak force evoked during the NMES session was 120 ± 26 N and corresponded to 30 ± 4% MVC (Fig. 2*B*).

Maximal voluntary contraction force

MVC significantly decreased by 26 ± 9% immediately after the damaging exercise and was still reduced by 20 ± 6% at D7 and 12 ± 6% at D14 (Table 1). At D21, MVC was not significantly different from the baseline value ($P = 0.083$).

Muscle volume and T_2

NMES-induced muscle activation. The MR acquisition was performed 259 ± 39 s after the NMES cessation. At this time, no significant increase in muscle volume was found (Table 1) whereas a significant T_2 increase was measured in RF (+13 ± 8%), VL (+14 ± 6%) and VI (+7 ± 4%)

Table 1. Maximal voluntary contraction force (MVC) and magnetic resonance imaging parameters of knee extensors assessed before (PRE), immediately after (POST), and 7 days (D7), 14 days (D14) and 21 days (D21) after the NMES session

		PRE	POST	D7	D14	D21
MVC (N)		408 ± 114	301 ± 87[a]	326 ± 94[a]	347 ± 102[a,b,c]	367 ± 100[b,c]
Muscle volume (cm^3)	VL	843 ± 144	878 ± 173	944 ± 186	849 ± 141	823 ± 132
	VM	776 ± 133	789 ± 135	795 ± 126	771 ± 123	767 ± 123
	VI	840 ± 156	844 ± 176	839 ± 170	845 ± 170	835 ± 163
	RF	255 ± 75	268 ± 77	265 ± 77	262 ± 77	258 ± 79
	SAR	174 ± 38	175 ± 41	180 ± 41	177 ± 40	175 ± 39
T_2 (ms)	VL	32.6 ± 0.7	37.0 ± 1.9[a]	44.0 ± 5.6[a]	38.2 ± 2.9[a,c]	36.7 ± 2.2[a,c]
	VM	32.9 ± 0.5	35.1 ± 1.4[a]	37.0 ± 2.5[a]	35.5 ± 1.5[a]	34.7 ± 1.1[a,c]
	VI	33.1 ± 0.7	33.9 ± 0.9	34.5 ± 1.2[a]	34.1 ± 0.8[a]	33.7 ± 0.7
	RF	32.4 ± 0.7	36.6 ± 2.3[a]	34.2 ± 1.6[a]	33.3 ± 1.0	32.9 ± 1.3
	SAR	32.4 ± 1.0	34.1 ± 1.5	36.0 ± 3.1[a]	34.9 ± 1.3[a]	33.9 ± 1.3[a]

Data are means ± SD. VL: vastus lateralis; VM: vastus medialis; VI: vastus intermedius; RF: rectus femoris; SAR: sartorius.
[a]Significantly different from PRE ($P < 0.05$),
[b]significantly different from POST ($P < 0.05$),
[c]significantly different from D7 ($P < 0.05$).

(Fig. 3). No significant T_2 change was found in other thigh muscles (Tables 1 and 2).

NMES-induced muscle damage. At D7, T_2 values were still elevated in RF (+6 ± 3%), SAR (+11 ± 11%), VI (+4 ± 4%), VL (+35 ± 17%) and VM (+12 ± 8%). These changes were still present at D14 for SAR (+8 ± 3%), VI (+3 ± 2%), VL (+17 ± 8%) and VM (+8 ± 5%) (Fig. 3). At D21, T_2 was still increased for the two muscles located beneath the stimulation electrodes (VL: +13 ± 7% and VM: +5 ± 4%, Table 1). No significant change was detected in other muscles (Table 2).

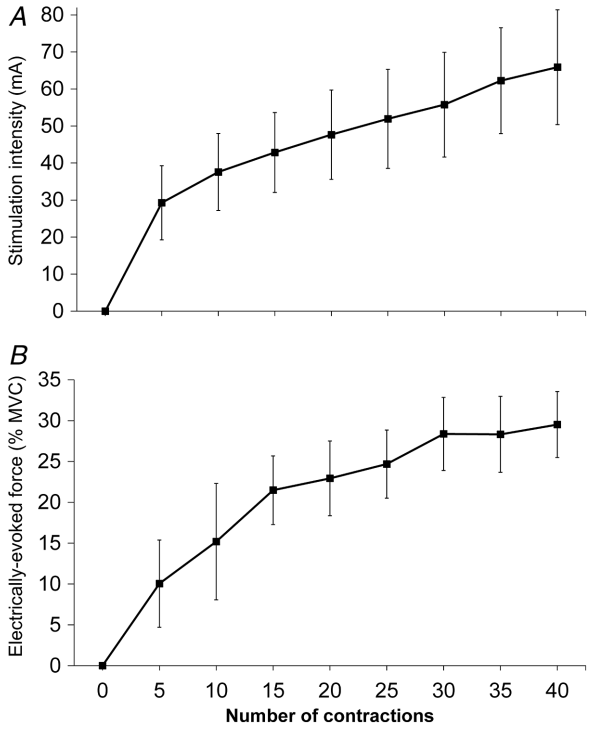

Figure 2. Changes in stimulation intensity (*A*) and electrically-evoked force (*B*) during the damaging neuromuscular electrical stimulation session (means ± SD)

Spatial normalization and statistical parametric mapping analyses

High DSC values were found for both intra-subject normalization (0.96 ± 0.02 [range: 0.86–0.99]) and inter-subject normalization (0.88 ± 0.07 [range: 0.46–0.96]). Very high scores were especially obtained on the main region of interest (i.e. quadriceps femoris muscles) for intra-subject and inter-subject normalization (0.97 ± 0.01 [range: 0.93–0.98] and 0.94 ± 0.01 [range: 0.88–0.96], respectively).

The SPM analysis showed a significant muscle T_2 increase at POST in the superficial parts of both VL and VM muscles (Fig. 4). At D7, D14 and D21, T_2 values were still elevated in the deep part of the VL muscle and superficial part of the VM muscle. The SPM analyses also demonstrated a significant T_2 decrease from D7 to D14 in the VL whereas no significant change was observed from D14 to D21.

T_2 quantification in deep and superficial parts of the VM and the VL

Localized T_2 changes were quantified in the superficial and deep parts of the VL and VM muscles (Table 3). While a significant activation (i.e. T_2 increase) of the whole VL and VM muscles was found ($P < 0.05$), this activation was

significantly higher in the superficial part, especially near the position of the stimulation electrodes (i.e. +17 ± 5% in the proximal part for the VL and +14 ± 7% in the distal part for the VM).

The highest T_2 change was quantified at D7 for both the VL and VM muscles (Table 3). Interestingly, deep and superficial parts did not display similar changes with a larger increase in the VM superficial part (+24 ± 16% *vs.* +9 ± 7% in the deep part) and in the VL deep part (+57 ± 24% *vs.* +38 ± 22% in the superficial part). No further difference was quantified between deep and superficial parts of both muscles at D14 and D21.

Discussion

On the basis of immediate and long lasting T_2 changes recorded after an isometric NMES session, the present results clearly demonstrated that muscle areas activated during the contractions can be spatially different from the damaged muscle regions. Muscle T_2 was increased immediately after the NMES session in the superficial parts of the VL and the VM whereas, on the basis of delayed T_2 increases at D7, D14 and D21, alterations were mainly identified in the VM superficial part and the VL deep part. One can then suggest that VM muscle fibres, activated during the NMES session, were damaged together with passive structural components within the VL muscle (e.g. connective tissues and/or costameres). Therefore, the localization of damage following NMES-induced isometric contractions are muscle specific and do not necessarily correspond to activation zones.

Muscle T_2 changes quantified immediately after the NMES session have been acknowledged as an indirect marker of muscle activation and used in order to identify muscle-activated areas during electrically-evoked contractions (Adams *et al.* 1993; Kinugasa *et al.* 2006; Jubeau *et al.* 2015; Fouré *et al.* 2017). Exercise-induced T_2 increase has been associated with an increased muscle volume and mainly related to an accumulation of intramuscular water from osmotically and/or hydrostatically driven fluid shifts (Meyer *et al.* 2001; Damon *et al.* 2002) and also to intracellular acidification (Louie *et al.* 2009). The SPM analyses clearly demonstrated a significant T_2 change in the superficial part of the stimulated muscles (i.e. VM and VL). This superficial activation of muscle areas located beneath the stimulation electrodes is consistent with the motor units' recruitment using NMES. This result does not support those from a previous MRI study indicating that NMES was related to a heterogeneous activation of the four muscles of the quadriceps femoris (Adams *et al.* 1993). Adams *et al.* used a thresholding approach in order to characterize muscle-activated areas (Adams *et al.* 1993). Considering the large inter-individual and intra-muscular T_2 variabilities, the corresponding results might have been misinterpreted. Combining T_2 mapping and SPM analyses, we were able to clearly demonstrate a superficial muscle activation of VM and VL muscles during the NMES session, especially beneath the stimulation electrodes, whereas Adams *et al.* did not clearly assess a specific localization of activated muscle area associated with their stimulation protocol. However, muscle activation patterns could have been different with the larger stimulation electrodes, pulse duration and the lower frequency used in the latter study (Adams *et al.* 1993).

Persistent T_2 changes recorded at D7, D14 and D21 were identified as muscle tissue alterations as previously described (Foley *et al.* 1999; Fouré *et al.* 2014, 2015*a*). Interestingly, muscle alterations were localized in the superficial areas of the VM whereas damage was found in the VL deep part. One can hypothesize that alterations detected in the superficial part of the VM could be related to a critical use of muscle fibres similar to what can be reported after muscle overuse. On the contrary, regarding the VL muscle, activated and damaged areas

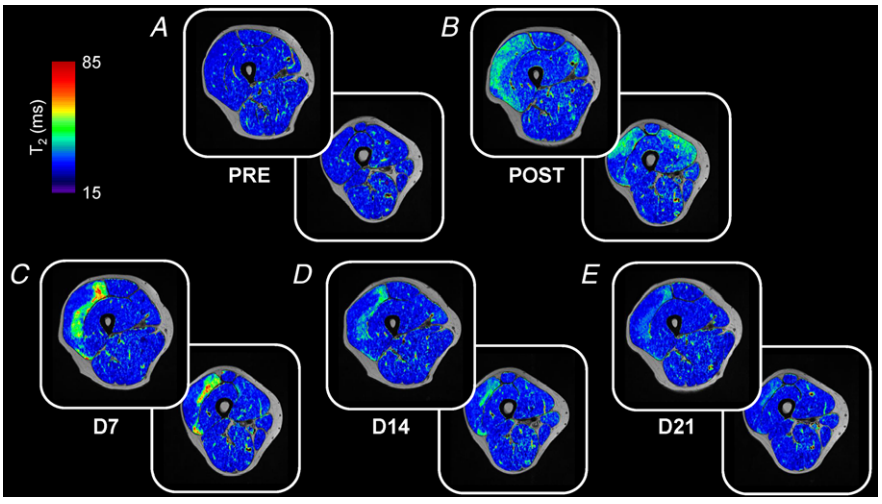

Figure 3. Comparison of muscle volume and T_2 mapping before (*A*), immediately after (*B*) and in the following days (from *C* to *E*) after the neuromuscular electrical stimulation session for a representative subject in a proximal and a distal slice
Muscle activation was determined by a comparison of muscle T_2 values obtained before (PRE) and immediately after (POST) the neuromuscular electrical stimulation session. Muscle damage was assessed from changes in T_2 at 7 days (D7), 14 days (D14) and 21 days (D21) after the damaging exercise in comparison to the baseline assessment (PRE). [Colour figure can be viewed at wileyonlinelibrary.com]

Table 2. MRI parameters assessed before (PRE), immediately after (POST), and 7 days (D7), 14 days (D14) and 21 days (D21) after NMES session

		PRE	POST	D7	D14	D21
Muscle volume (cm^3)	GR	156 ± 28	152 ± 29	154 ± 28	159 ± 32	157 ± 31
	ADD-L	154 ± 36	155 ± 43	154 ± 37	158 ± 36	158 ± 32
	ADD-M	631 ± 101	631 ± 119	634 ± 112	642 ± 97	631 ± 96
	BF-S	165 ± 56	160 ± 53	162 ± 54	166 ± 54	166 ± 54
	BF-L	391 ± 60	386 ± 64	390 ± 62	393 ± 59	392 ± 61
	ST	295 ± 40	289 ± 44	294 ± 42	296 ± 42	296 ± 43
	SM	442 ± 135	436 ± 124	439 ± 127	441 ± 126	443 ± 125
T_2 (ms)	GR	31.7 ± 0.9	31.7 ± 1.3	31.9 ± 0.9	32.2 ± 1.0	32.0 ± 1.3
	ADD-L	33.3 ± 1.1	33.6 ± 1.3	33.7 ± 0.9	34.1 ± 1.2	34.0 ± 1.2
	ADD-M	33.8 ± 0.7	33.8 ± 1.3	34.3 ± 1.0	34.6 ± 0.9	34.2 ± 0.9
	BF-S	32.2 ± 1.0	32.1 ± 1.4	32.6 ± 1.1	33.1 ± 1.3	32.7 ± 1.0
	BF-L	32.4 ± 0.8	32.2 ± 1.0	32.8 ± 0.8	33.3 ± 1.1	32.8 ± 0.7
	ST	32.0 ± 1.0	31.6 ± 1.0	32.0 ± 0.6	32.5 ± 1.2	32.2 ± 0.8
	SM	33.0 ± 0.8	32.6 ± 1.0	33.1 ± 0.7	33.5 ± 1.0	33.1 ± 0.8

Data are means ± SD. GR: gracilis, ADD-L: adductor longus, ADD-M: adductor magnus, BF-S: biceps femoris short head, BF-L: biceps femoris long head, ST: semitendinosus, SM: semimembranosus.

were spatially different thereby suggesting that intramuscular shear stress could be the accounting factor of the damage occurring during the NMES session as previously suggested (Fouré *et al.* 2015*a*,b). In other words, tissues other than active muscle fibres such as connective tissues and/or intracellular structural elements such as costameres could be altered during damaging contractions (Crameri *et al.* 2007; Mackey *et al.* 2011; Lieber, 2018). For instance, Mackey *et al.* (2008) clearly observed desmin-negative fibres in electrically stimulated muscles as compared to voluntary-activated muscles. Further studies would be warranted in order to investigate the behaviour of muscle fibres and connective tissues during isometric electrically-evoked contractions leading to damage. In agreement with previous studies, MVC dropped after the NMES session likely as a result of muscle damage as

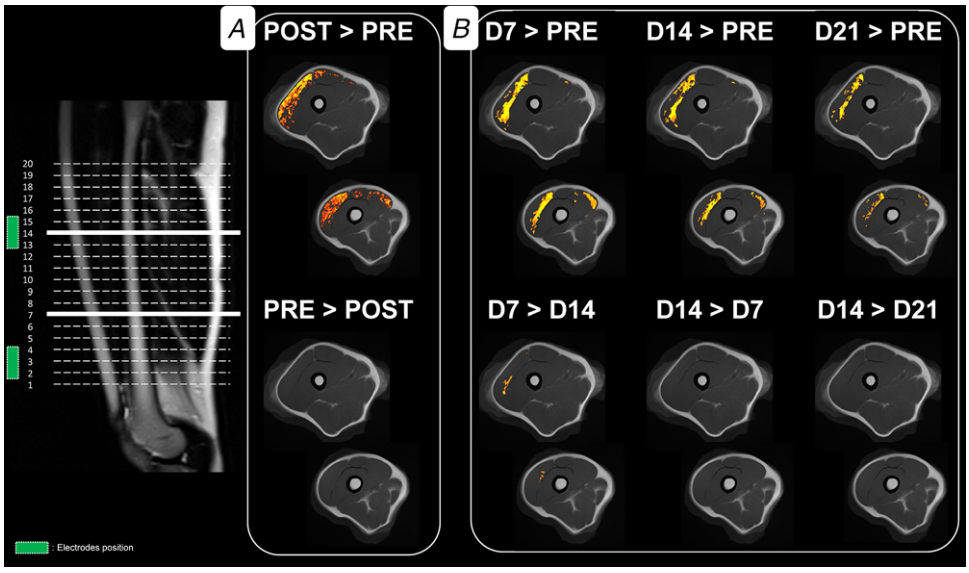

Figure 4. Statistical parametric mapping analyses for T_2 increase in the thigh muscles between baseline (PRE) and acquisitions performed immediately after (POST) the damaging exercise (*A*), and 7 days (D7), 14 days (D14) and 21 days (D21) after the neuromuscular electrical stimulation session (*B*)
Comparisons were performed with SPM12 software ($P < 0.0001$ and a cluster size >100 voxels). The colour scale (from red to yellow) represents the degree of significance (low to high). Results of the statistical analysis displayed on two slices (i.e. a distal and a proximal slice represented by thick bars on the sagittal slice on the left) were overlaid on the T_1-weighted axial images of the co-registration template including the entire experimental population. [Colour figure can be viewed at wileyonlinelibrary.com]

Table 3. Muscle T_2 values in deep and superficial parts along the vastus lateralis and vastus medialis before (PRE), immediately after (POST) and 7 days (D7), 14 days (D14) and 21 days (D21) after NMES-induced muscle damage

		VL		VM	
		Sup	Deep	Sup	Deep
PRE	Proximal	32.5 ± 1.2	32.5 ± 1.2	33.0 ± 1.0	32.4 ± 0.8
	Central	31.2 ± 0.8	31.9 ± 0.8	32.4 ± 0.6	32.3 ± 0.8
	Distal	32.4 ± 1.0	33.1 ± 1.0	33.6 ± 0.5	33.5 ± 0.8
	Whole muscle	**32.2 ± 1.0**	**32.5 ± 1.0**	**33.3 ± 0.6**	**32.9 ± 0.7**
POST	Proximal	38.2 ± 1.7[a,#]	36.1 ± 1.4[a]	34.5 ± 1.5[a]	33.3 ± 1.0[a]
	Central	37.0 ± 2.0[a]	36.7 ± 1.7[a]	35.6 ± 2.0[a,#]	33.8 ± 1.6[a]
	Distal	37.6 ± 2.1[a]	38.4 ± 2.2[a]	38.4 ± 2.1[a,#]	36.1 ± 1.7[a]
	Whole muscle	**37.8 ± 1.7[a]**	**36.6 ± 1.4[a]**	**36.9 ± 1.9[a,#]**	**34.9 ± 1.4[a]**
D7	Proximal	45.3 ± 8.0[a]	51.2 ± 8.9[a]	37.1 ± 3.6[a,#]	33.5 ± 1.1
	Central	44.3 ± 7.1[a,#]	52.8 ± 6.8[a]	40.9 ± 5.7[a,#]	34.7 ± 2.4
	Distal	44.3 ± 6.7[a]	50.3 ± 10.0[a]	42.7 ± 5.6[a,#]	37.6 ± 3.8[a]
	Whole muscle	**44.6 ± 7.0[a,#]**	**51.1 ± 7.8[a]**	**41.1 ± 5.0[a,#]**	**35.8 ± 2.6[a]**
D14	Proximal	37.7 ± 3.0[a,b]	40.9 ± 3.7[a,b]	35.7 ± 2.2[a]	33.5 ± 1.4
	Central	36.9 ± 3.1[a,b]	41.3 ± 3.4[a,b]	36.9 ± 2.5[a,b]	33.8 ± 1.5
	Distal	37.1 ± 3.3[a,b]	39.4 ± 4.4[a,b]	38.6 ± 2.0[a,b]	36.0 ± 2.2
	Whole muscle	**37.4 ± 2.8[a,b]**	**40.7 ± 3.4[a,b]**	**37.6 ± 1.9[a,b]**	**34.8 ± 1.6**
D21	Proximal	36.4 ± 2.5[a,b]	38.4 ± 3.0[a,b]	34.4 ± 1.3[b]	32.9 ± 1.0
	Central	35.3 ± 2.4[b]	38.6 ± 2.8[a,b]	35.5 ± 2.4[a,b]	33.1 ± 1.1
	Distal	35.6 ± 1.8[a,b]	37.9 ± 3.1[a,b]	37.1 ± 1.9[a,b]	35.3 ± 1.7
	Whole muscle	**36.0 ± 2.3[b]**	**38.4 ± 2.8[a,b]**	**36.2 ± 1.8[a,b]**	**34.1 ± 1.2**

Data are means ± SD (ms). VL: vastus lateralis; VM: vastus medialis. Sup: superficial part of the muscle, Deep: deep part of the muscle, [a]Significantly different from PRE ($P < 0.05$), [b]significantly different from D7 ($P < 0.05$), [#]significantly different from deep part ($P < 0.05$).

previously reported (Aldayel *et al.* 2010*a*,*b*; Nosaka *et al.* 2011; Paulsen *et al.* 2012). At D7 and D14, MVC did not reach the baseline values, similar to what occurred for muscle T_2 until D21. Therefore, it could be emphasized that the isometric NMES exercise used in the present study generated severe muscle damage (Paulsen *et al.* 2012).

It is noteworthy that muscle volume was unchanged for each measurement in the present study. Therefore, no significant swelling/oedema occurred as an immediate and a delayed (i.e. from D7 to D21) result of the NMES session. However, the oedema related to exercise-induced muscle damage has been commonly reported as peaking 2–4 days after a damaging exercise (Fouré *et al.* 2015*a*). On that basis, we can hypothesize that oedema was already resorbed at D7. In addition, T_2 change was detected at POST in superficial thigh muscles thereby illustrating that VL, VM and RF were the main muscles involved in force production during the NMES session. However, the increased T_2 value quantified in the RF muscle at POST could be due to a potential activation of some RF nerve branches located in the vicinity of the VL and VM muscles and/or to a potential diffusion of water from VM and VL compartments to the RF one. In addition, a slight involvement of the other knee extensor muscles cannot be ruled out considering the significant changes in T_2 for SAR, VI and RF from D7 to D21.

From a methodological point of view, muscle tissue alterations were detected from robust data analyses including image co-registrations and statistical analyses (Fouré *et al.* 2015*b*, 2018). Such an approach overcomes the inter-subject variability and is not based on the arbitrary choice of a threshold (Adams *et al.* 1993; Kinugasa *et al.* 2005, 2011) to determine activation or alteration based on T_2 changes. This methodology allows the detection of spatially determined significant difference in T_2 maps over an experimental group. It should be noteworthy that volume and T_2 quantifications were performed in the raw serial images on the basis of a specific parcellation determined from the SPM results. Regarding the NMES session, muscle activation pattern would have been different by changing stimulation electrode size and other parameters such as frequency or pulse duration as previously displayed by change in muscle T_2 (Adams *et al.* 1993; Gorgey *et al.* 2006). This difference in muscle activation pattern can then influence the localization and the extent of muscle damage associated with the NMES session. However, the major result of the study still

illustrated difference regarding localization of activated and damaged muscle areas within the VL. During the NMES session, the intensity was manually increased until a mean relative force was produced during the NMES session of about 25–30% MVC as previously reported (Fouré *et al.* 2015*b*). Although inter-individual variability was found in the relative evoked force during the first contractions of the NMES session, a low coefficient of variation (∼15%) was assessed considering the last 25 contractions. Therefore, a similar involvement of relative muscle volume can be assumed among individuals.

Overall, based on the combination of image co-registration and a robust statistical analysis, the present results demonstrated that activated and altered skeletal muscle areas can be spatially different after an isometric NMES session. Additional investigations are needed in order to more specifically assess the exact involvement of connective tissue in exercise-induced muscle alterations. The present methodological approach might be useful to accurately determine the localization and extent of muscle damage following voluntary contractions and for the clinical assessment of tissue alterations/rehabilitation in athletes and/or in patients with neuromuscular diseases.

References

Adams GR, Harris RT, Woodard D & Dudley GA (1993). Mapping of electrical muscle stimulation using MRI. *J Appl Physiol (1985)* **74**, 532–537.

Aldayel A, Jubeau M, McGuigan M & Nosaka K (2010*a*). Comparison between alternating and pulsed current electrical muscle stimulation for muscle and systemic acute responses. *J Appl Physiol (1985)* **109**, 735–744.

Aldayel A, Jubeau M, McGuigan MR & Nosaka K (2010*b*). Less indication of muscle damage in the second than initial electrical muscle stimulation bout consisting of isometric contractions of the knee extensors. *Eur J Appl Physiol* **108**, 709–717.

Crameri RM, Aagaard P, Qvortrup K, Langberg H, Olesen J & Kjaer M (2007). Myofibre damage in human skeletal muscle: effects of electrical stimulation *versus* voluntary contraction. *J Physiol* **583**, 365–380.

Damon BM, Gregory CD, Hall KL, Stark HJ, Gulani V & Dawson MJ (2002). Intracellular acidification and volume increases explain R_2 decreases in exercising muscle. *Magn Reson Med* **47**, 14–23.

Fleckenstein JL, Weatherall PT, Parkey RW, Payne JA & Peshock RM (1989). Sports-related muscle injuries: evaluation with MR imaging. *Radiology* **172**, 793–798.

Foley JM, Jayaraman RC, Prior BM, Pivarnik JM & Meyer RA (1999). MR measurements of muscle damage and adaptation after eccentric exercise. *J Appl Physiol (1985)* **87**, 2311–2318.

Fouré A, Duhamel G, Vilmen C, Bendahan D, Jubeau M & Gondin J (2017). Fast measurement of the quadriceps femoris muscle transverse relaxation time at high magnetic field using segmented echo-planar imaging. *J Magn Reson Imaging* **45**, 356–368.

Fouré A, Duhamel G, Wegrzyk J, Boudinet H, Mattei JP, Le Troter A, Bendahan D & Gondin J (2015*a*). Heterogeneity of muscle damage induced by electrostimulation: a multimodal MRI study. *Med Sci Sports Exerc* **47**, 166–175.

Fouré A, Le Troter A, Guye M, Mattei JP, Bendahan D & Gondin J (2015*b*). Localization and quantification of intramuscular damage using statistical parametric mapping and skeletal muscle parcellation. *Sci Rep* **5**, 18580.

Fouré A, Nosaka K, Wegrzyk J, Duhamel G, Le Troter A, Boudinet H, Mattei JP, Vilmen C, Jubeau M, Bendahan D & Gondin J (2014). Time course of central and peripheral alterations after isometric neuromuscular electrical stimulation-induced muscle damage. *PLoS One* **9**, e107298.

Fouré A, Ogier AC, Le Troter A, Vilmen C, Feiweier T, Guye M, Gondin J, Besson P & Bendahan D (2018). Diffusion properties and 3D architecture of human lower leg muscles assessed with ultra-high-field-strength diffusion-tensor MR imaging and tractography: reproducibility and sensitivity to sex difference and intramuscular variability. *Radiology* **287**, 592–607.

Gorgey AS, Mahoney E, Kendall T & Dudley GA (2006). Effects of neuromuscular electrical stimulation parameters on specific tension. *Eur J Appl Physiol* **97**, 737–744.

Gregory CM & Bickel CS (2005). Recruitment patterns in human skeletal muscle during electrical stimulation. *Phys Ther* **85**, 358–364.

Jubeau M, Le Fur Y, Duhamel G, Wegrzyk J, Confort-Gouny S, Vilmen C, Cozzone PJ, Mattei JP, Bendahan D & Gondin J (2015). Localized metabolic and T2 changes induced by voluntary and evoked contractions. *Med Sci Sports Exerc* **47**, 921–930.

Kinugasa R, Kawakami Y & Fukunaga T (2005). Muscle activation and its distribution within human triceps surae muscles. *J Appl Physiol (1985)* **99**, 1149–1156.

Kinugasa R, Kawakami Y & Fukunaga T (2006). Mapping activation levels of skeletal muscle in healthy volunteers: an MRI study. *J Magn Reson Imaging* **24**, 1420–1425.

Kinugasa R, Kawakami Y, Sinha S & Fukunaga T (2011). Unique spatial distribution of *in vivo* human muscle activation. *Exp Physiol* **96**, 938–948.

Le Troter A, Foure A, Guye M, Confort-Gouny S, Mattei JP, Gondin J, Salort-Campana E & Bendahan D (2016). Volume measurements of individual muscles in human quadriceps femoris using atlas-based segmentation approaches. *MAGMA* **29**, 245–257.

Lieber RL (2018). Biomechanical response of skeletal muscle to eccentric contractions. *J Sport Health Sci* **7**, 294–309.

Louie EA, Gochberg DF, Does MD & Damon BM (2009). Transverse relaxation and magnetization transfer in skeletal muscle: effect of pH. *Magn Reson Med* **61**, 560–569.

Mackey AL, Bojsen-Moller J, Qvortrup K, Langberg H, Suetta C, Kalliokoski KK, Kjaer M & Magnusson SP (2008). Evidence of skeletal muscle damage following electrically stimulated isometric muscle contractions in humans. *J Appl Physiol (1985)* **105**, 1620–1627.

Mackey AL, Brandstetter S, Schjerling P, Bojsen-Moller J, Qvortrup K, Pedersen MM, Doessing S, Kjaer M, Magnusson SP & Langberg H (2011). Sequenced response of extracellular matrix deadhesion and fibrotic regulators after muscle damage is involved in protection against future injury in human skeletal muscle. *FASEB J* **25**, 1943–1959.

Maffiuletti NA (2010). Physiological and methodological considerations for the use of neuromuscular electrical stimulation. *Eur J Appl Physiol* **110**, 223–234.

Meyer RA, Prior BM, Siles RI & Wiseman RW (2001). Contraction increases the T_2 of muscle in fresh water but not in marine invertebrates. *NMR Biomed* **14**, 199–203.

Morgan DL (1990). New insights into the behavior of muscle during active lengthening. *Biophys J* **57**, 209–221.

Nosaka K, Aldayel A, Jubeau M & Chen TC (2011). Muscle damage induced by electrical stimulation. *Eur J Appl Physiol* **111**, 2427–2437.

Ogier A, Sdika M, Fouré A, Le Troter A & Bendahan D (2017). Individual muscle segmentation in MR images: A 3D propagation through 2D non-linear registration approaches. *Conf Proc IEEE Eng Med Biol Soc* **2017**, 317–320.

Paulsen G, Mikkelsen UR, Raastad T & Peake JM (2012). Leucocytes, cytokines and satellite cells: what role do they play in muscle damage and regeneration following eccentric exercise? *Exerc Immunol Rev* **18**, 42–97.

Proske U & Allen TJ (2005). Damage to skeletal muscle from eccentric exercise. *Exerc Sport Sci Rev* **33**, 98–104.

Zou KH, Warfield SK, Bharatha A, Tempany CM, Kaus MR, Haker SJ, Wells WM 3rd, Jolesz FA & Kikinis R (2004). Statistical validation of image segmentation quality based on a spatial overlap index. *Acad Radiol* **11**, 178–189.

Additional information

Competing interests

The authors have no conflicts of interest to disclose.

Authors contributions

Experiments were performed at the 'Centre d'Exploration Métabolique par Résonance Magnétique' (CEMEREM–UMR 7339, AMU, CNRS, APHM). Concerning authors' contributions: A.F. and J.G. contributed to the conception or design of the work; A.F., A.LeT., A.C.O., M.G., J.G. and D.B. contributed to the acquisition, analysis or interpretation of data for the work; A.F., A.LeT., A.C.O., M.G., J.G. and D.B. contributed to drafting the work or revising it critically for important intellectual content. All the authors approved the final version of the manuscript, agreed to be accountable for all aspects of the work in ensuring that questions related to the accuracy or integrity of any part of the work are appropriately investigated and resolved. All persons designated as authors qualify for authorship, and all those who qualify for authorship are listed

Funding

This study was supported by the Centre National de la Recherche Scientifique (CNRS UMR 7339) and the Assistance Publique des Hôpitaux de Marseille (APHM).

Acknowledgements

The authors thank Véronique Gimenez for her help and all the subjects who participated in the present study.